rocscience

RS2

Unsaturated Soil Mechanics

Examples

© 2022 Rocscience Inc.

Table of Contents

1. Effect of Concentrated Rainfall on Slope Stability with RS2

1.1. Introduction

Concentrated rainfall has been known to induce landslides due to the reduction of soil suction and subsequent loss of shear strength. As rain infiltrates the soil it replaces the air-filled pores in the unsaturated zone with water, increasing pore water pressure and decreasing effective stress, resulting in diminished strength.

Regions that experience monsoon seasons such as Nepal are particularly susceptible to rain-induced slope failure due to the sudden loss of soil suction. This phenomenon has been studied in the paper by Pradhan et al. (2022), which investigated a slope with a road cut in Nepal that failed in July 2018 after a period of high intensity rainfall. A back-analysis was performed to predict the factor of safety over a period of 12 days prior to the landslide, clearly indicating a correlation between safety factor reduction and rainfall infiltration.

The analysis was replicated in RS2, comparing the safety factor variation and pore water pressure contour at time of failure to the results of the paper. The paper presents two slope cases, one with a road cut and one without. Since the effect of road cut is not considered in this example, only the case of the slope with the road cut was examined in RS2.

1.2. Theory

A coupled hydro-mechanical analysis was conducted based on Biot's theory of consolidation (1941) which allows for the interdependency between pore pressure and deformation to be factored into the model.

The mechanical behavior was modelled using Bishop's single effective stress approach (1959) for unsaturated soil, which defines effective stress σ' as a relation between the total stress σ and suction $(u_a - u_w)$.

$$\sigma' = (\sigma - u_a) + \chi(u_a - u_w) \quad (1.1)$$

The above equation can often be simplified to the following form, where the suction coefficient χ is equivalent to the effective degree of saturation S_e and pore air pressure u_a is considered negligible.

$$\sigma' = \sigma - S_e u_w \quad (1.2)$$

$$S_e = \frac{S - S_r}{S_s - S_r} \quad (1.3)$$

Where u_w is the pore water pressure, S is the degree of saturation, S_r is the degree of saturation at residual state, and S_s is the degree of saturation at fully saturated state.

The unsaturated hydraulic behavior was modelled using the van Genuchten model (1980) which defines a relationship between the volumetric water content and matric suction and estimates the unsaturated soil conductivity using a set of curve fitting parameters.

$$\theta_e = \frac{\theta - \theta_r}{\theta_s - \theta_r} = \frac{1}{[1 + (\alpha\psi)^n]^m} \tag{1.4}$$

$$k = k_s k_r = k_s \theta_e{}^l \left[1 - \left(1 - \theta_e{}^{1/m}\right)^m\right]^2 \tag{1.5}$$

Where θ is the volumetric water content, θ_e is the normalized volumetric water content, θ_r is the residual volumetric water content, θ_s is the saturated volumetric water content, ψ is the matric suction head, k is the coefficient of permeability, k_s is the saturated coefficient of permeability, k_r is the relative permeability, and α, n, m, and l are the curve fitting parameters where $m = 1 - 1/n$.

The saturated volumetric water content θ_s is commonly assumed to be equivalent to porosity n, which can be calculated from the void ratio e.

$$n = \frac{e}{1 + e} \tag{1.6}$$

1.3. Model Geometry

During the 12-day period (271 h), 13 critical points were modelled and analyzed in RS2. For all 13 models, they share the same geometry, initial conditions, steady-state conditions, and material properties.

Geometry

The model geometry consists of a slope with a steep road cut. It contains 12938 mesh elements and 26151 mesh nodes, with a finer mesh defined around the road cut to capture the expected deformation more accurately. The top three soil layers are all 0.5m thick.

Initial Conditions and Steady State

The initial phreatic surface was assumed to be 15m below the surface as shown in Figure 1.1 (left). The initial pore water pressures were then generated by applying constant influx to the surface for 5 years to achieve steady state. After the steady state is reached, as shown in Figure 1.1 (right) below, the transient rainfall boundary condition was then applied for 12 days until slope failure.

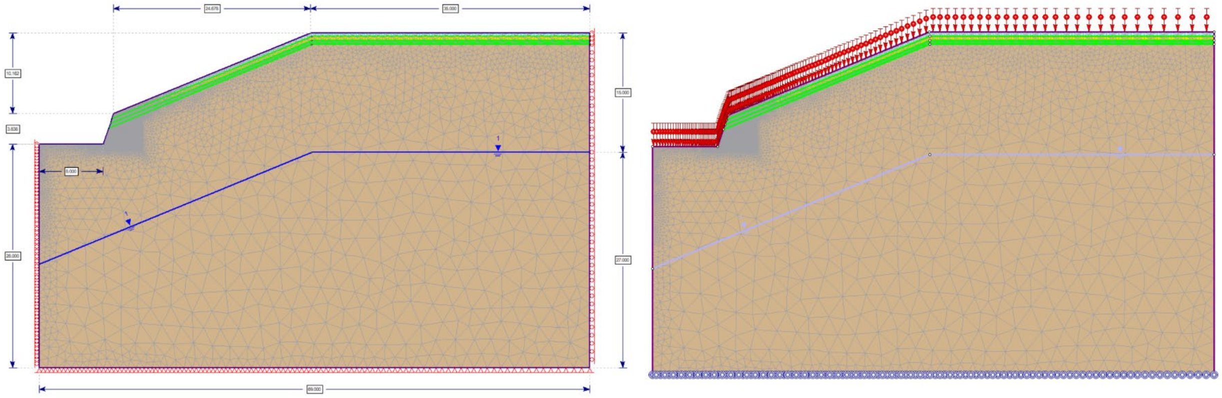

Figure 1.1: initial state (left), applied transient rainfall (right)

1.4. Material Properties

The material properties used in the model are as shown in Table 1.1. Note that the unsaturated behavior is set to “Single Effective Stress” with the “Bishop” method in the material properties. Without these parameters set, the model is unstable in the initial stage since the suction effects are not accounted for in effective stress calculation process.

Table 1.1: Material and hydraulic properties

Soil Layer	1	2	3	4
Unsaturated unit weight (kN/m3)	17.4	17.4	19.1	20.2
Saturated unit weight (kN/m3)	18.4	18.4	20.1	21.2
Porosity	0.5098	0.43503	0.36306	0.36306
Elastic modulus (MPa)	6	7	7	7
Poisson's ratio	0.35	0.35	0.35	0.35
Failure Criterion	Mohr-Coulomb			
Material Type	Plastic			
Peak cohesion (kPa)	3	3	3	3
Peak angle of shearing resistance (degrees)	36	36	36	36
Residual cohesion (kPa)	0	0	0	0
Unsaturated Behavior	Single Effective Stress			
Single Effective Stress Method	Bishop			
Saturated permeability (m/s)	5.80E-07	2.70E-07	2.60E-07	2.40E-07

Curve fitting parameters (wetting)				
α (1/m)	0.272	0.226	0.14	0.14
n	1.315	1.405	1.405	1.405
m	0.239	0.288	0.288	0.288

1.5. Results

The paper's slope stability results were computed in PLAXIS 2D using the shear strength reduction method. The SRF's from the paper and the RS2 analysis are plotted in Figure 1.2, along with the hourly rainfall data for the 12-day period before slope failure. The graph displays a clear correlation between rain infiltration and factor of safety. Over periods of high intensity rainfall, the factor of safety declines rapidly, and during dry periods the factor of safety recovers at a slower rate. The factor of safety declines to 1 during hour 271, which corresponds to the observed time of failure for the slope. SRF values were obtained in RS2 at critical points during the 12-day period, and closely follow the variations obtained in the paper.

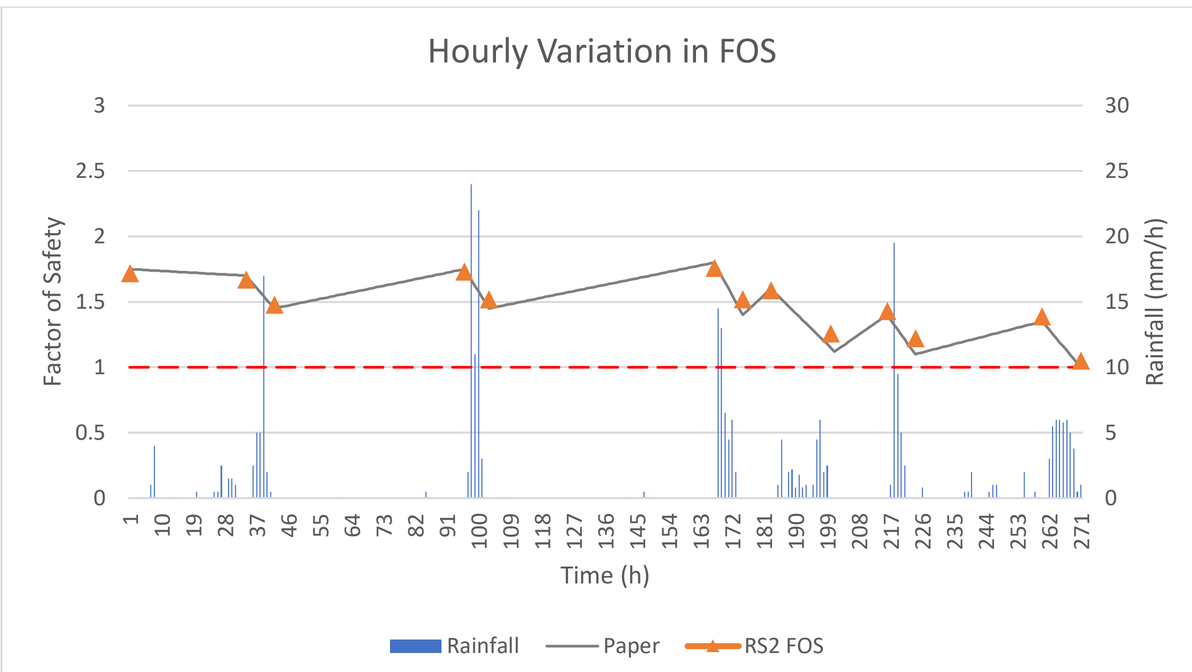

Figure 1.2: Factor of safety variations with time

Figure 1.3 displays suction contours at time of failure obtained from PLAXIS 2D (left) and RS2 (right). Both graphs show a thin layer of zero suction pressure near the surface of the slope due to the infiltration of rainwater. The reduction of suction in this region results in the decrease of the mean effective stress, thus the factor of safety was reduced as shown in Figure 1.3.

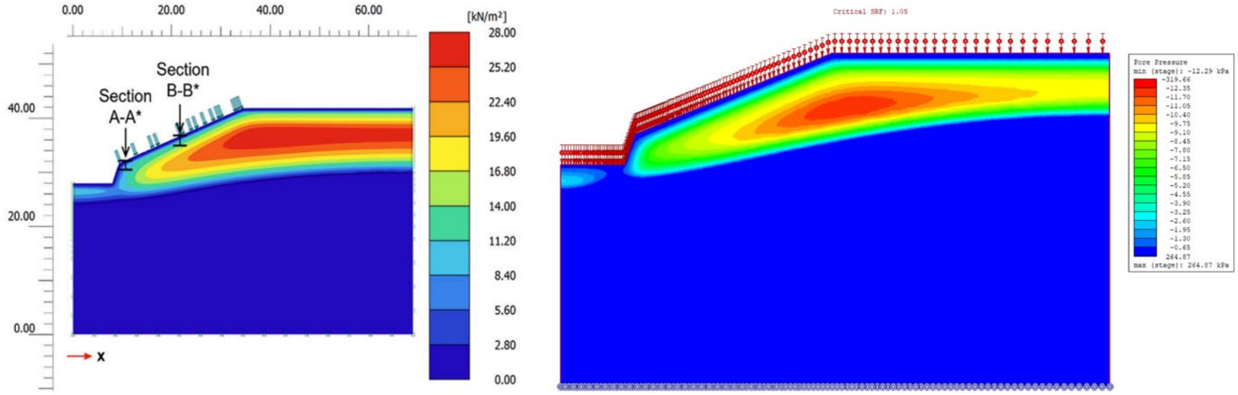

Figure 1.3: Suction contours at time of failure, PLAXIS 2D (left) RS2 (right)

Figure 1.4 displays the total displacement contours at time of failure. The RS2 graph (right) closely imitates the failure region in the graph from PLAXIS 2D (left).

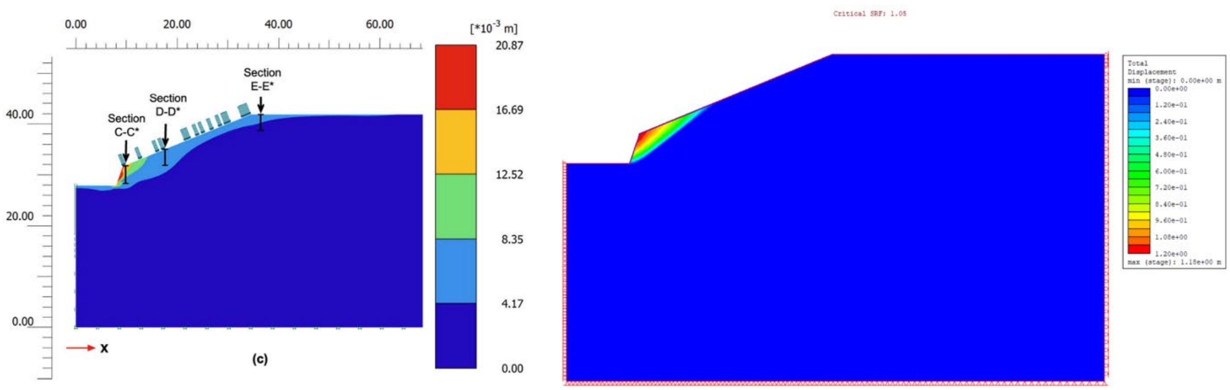

Figure 1.4: Total displacement contours at time of failure, PLAXIS 2D (left) RS2 (right)

1.6. References

Biot, M.A. (1941). General theory of three-dimensional consolidation. *Journal of Applied Physics, 12, pp.155-164.*

Bishop, A.W. (1959). The principle of effective stress. *Tecknish Ukeblad, 106, pp. 859-863.*

Pradhan, S., Toll, D.G., Rosser, N.J., and Brain, M.J. (2022). An investigation of the combined effect of rainfall and road cut on landsliding. *Engineering Geology 307 (2022) 106787.*

van Genuchten, M.T. (1980). A closed-form equation for predicting the hydraulic conductivity of unsaturated soils. *Soil Science Society of America Journal, 44, pp. 892-898.*